Laser-induced micron and submicron ordering effects in quasi-percolated nanostructured silver thin films

2009 Nanotechnology 20 355304

(http://iopscience.iop.org/0957-4484/20/35/355304)

Nanotechnology **20** (2009) 355304 (6pp) doi:10.1088/0957-4484/20/35/355304

Laser-induced micron and submicron ordering effects in quasi-percolated nanostructured silver thin films

E Haro-Poniatowski[1,3], J C Alonso-Huitrón[1,4], C Acosta-Zepeda[1], M C Acosta-García[2] and N Batina[2]

[1] Departamento de Física, Universidad Autónoma Metropolitana Iztapalapa, Avenida San Rafael Atlixco No. 186 Colonia Vicentina, CP 09340 México DF, Mexico
[2] Departamento de Química, Universidad Autónoma Metropolitana Iztapalapa, Avenida San Rafael Atlixco No. 186 Colonia Vicentina, CP 09340 México DF, Mexico

E-mail: haro@xanum.uam.mx

Received 6 April 2009, in final form 4 July 2009
Published 11 August 2009
Online at stacks.iop.org/Nano/20/355304

Abstract

Quasi-percolated nanostructured silver thin films are used as the starting morphology for inducing simultaneously changes in shape and ordering effects by laser irradiation. The complex fingered nanostructures are transformed into nanospheres which in turn are arranged in micro-circular patterns when irradiated through a pinhole. These transformations are characterized by transmission electron microscopy and atomic force microscopy. The observed effects are explained using Fresnel diffraction theory. Good agreement with the experimental results is obtained. These results suggest that precise patterning engineering can be achieved through control of the spatial parameters such as the pinhole diameter and the distance from the mask to the sample.

(Some figures in this article are in colour only in the electronic version)

1. Introduction

The formation of controlled patterns at the micron and submicron level is important for the fabrication of different devices such as sensors or memories among others. Several approaches (chemical, lithographic) have been developed which lead to patterns having different shapes and sizes. In many cases these techniques are often complicate and time-consuming. Simultaneously patterning procedures are constantly evolving and achieving structures which are smaller and smaller; as an example, very recently nanoscale circular patterns of the order of 13 nm have been achieved using template self-assembly of diblock copolymers [1]. An interesting fast and simple alternative is to use laser light in order to transform matter at the nanometer scale. Laser-induced changes in size and morphology in noble metal thin films have been reported previously [2]. Furthermore the possibility of changing selectively the size, in different surroundings, of the nanoparticles and control the corresponding distribution has also been demonstrated [3–6]. In a previous work, we have shown that it is possible, within the same process, to induce both morphological changes and submicron patterning of metallic films at the percolation transition using a light structured illumination field to irradiate the sample [7]. Transition zones between transformed and untransformed regions were of the order of a few tens of nanometers. This technique has been referred to recently as diffraction-aided laser-induced microstructuring (DLAM) and used to pattern with a razor edge TiO_2 thin films deposited on glass [8]. A similar procedure has been used for the fabrication of ordered arrays of silicon cones by optical diffraction in ultrafast etching [9]. A different approach leading to ordered arrays of gold nanoparticles (gratings) has been proposed recently. This technique relies on the coupling of light into waveguided modes through plasmons in gold nanoparticles deposited on a membrane [10]. As in the present experiments the starting morphology are noble metal films close to the percolation state. Very recently we have used a single slit in

[3] Author to whom any correspondence should be addressed.
[4] Permanent address: Instituto de Investigaciones en Materiales, Universidad Nacional Autónoma de México, Coyoacán 04510, AP 70360 México DF, Mexico.

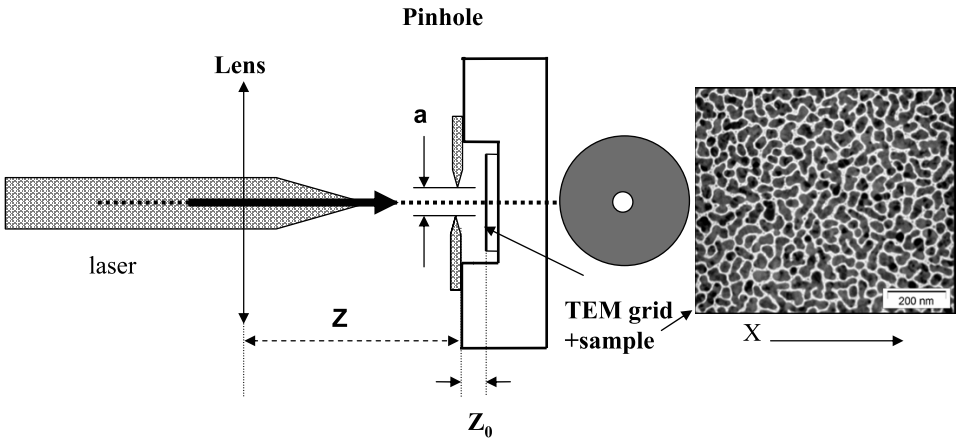

Figure 1. Experimental set-up for irradiating the samples. The starting quasi-percolated nanostructured silver thin film is shown on the right-hand side, the scale bar indicates 200 nm. The pinhole has a diameter of 60 μm and is placed at a distance of 300 μm from the sample.

order to produce by DLAM parallel bands of ordered silver nanoparticles [11]. Furthermore complex structured light fields can be produced with periodic masks such as phase mask diffraction gratings or a metallic square grid commonly used in transmission electron microscopy (TEM) [7, 12]. TEM is a powerful tool to study the morphology and structure of nanometric particles: however, in most of the cases it provides a two-dimensional characterization. On the other hand, atomic force microscopy (AFM) characterization gives three-dimensional information which is essential to understand the photo-transformation processes involved in laser irradiation. In the present work we show, starting with a quasi-percolated film morphology and using a diffractive mask, how to obtain an ordered pattern of silver nanoparticles. The diffractive mask is a 60 μm pinhole. The obtained diffraction pattern is imprinted in the quasi-percolated silver thin film. In the high intensity regions which in this case are rings the nanostructures are transformed into silver nanoparticles with sizes ranging from 10 to 100 nm. The observed effects are explained with Fresnel diffraction theory and a good agreement between theory and experiment is obtained. This opens up the possibility to control precisely the patterning effects through the spatial parameters characterizing the mask and its distance to the sample.

2. Experimental details

The starting quasi-percolated Ag films were prepared by pulsed laser ablation (PLA), using 15 000 shots of a Q-switched Nd:YAG laser providing 5 mJ pulses of 10 ns duration with a repetition rate of 5 Hz, at a wavelength of $\lambda = 355$ nm and at an average fluence of 0.64 J cm^{-2}. The PLA process was carried out in vacuum ($P \approx 1 \times 10^{-5}$ Torr). The substrates were Cu TEM (transmission electron microscopy) support grids covered with a carbon film. A detailed description of the experimental conditions is given elsewhere [13]. The morphology of the quasi-percolated films deposited on the TEM grids and the mean sizes of the Ag nanoparticles were examined by transmission electron microscopy (TEM) and atomic force microscopy (AFM). The experimental set-up used to irradiate the samples is shown in figure 1. For the present experiments we have used a quasi-percolated thin film shown on the right-hand side of figure 1. The sample was irradiated through a diffractive device, which in the present case was a circular aperture with a diameter a of 60 μm. The same Nd:YAG laser used for the pulsed laser deposition was used to irradiate in air the nanostructured samples at the same wavelength (355 nm). A focusing lens was placed in the laser beam to control the energy density. Since the irradiated samples were prepared on TEM grids, they were immediately observed after irradiation by electron microscopy and atomic force microscopy.

3. Results and discussion

As mentioned before we have irradiated a sample which is in a quasi-percolated state. This morphology is crucial in order to obtain the results reported here since, as stated previously, the fingered nanostructures will be the precursor particles which, upon irradiation, will transform into spherical nanoparticles. In a previous work we have studied the morphological changes as a function of the increasing energy density [7]. Below a minimum value, no modifications were detected on the sample as compared with the initial morphology. Two types of morphological changes were found; in the first type which occurred at an energy threshold F_{th1} the nanoparticles remained with similar irregular shapes: however, the characteristic distance between them (i.e. their average separation) increased. For higher fluences, a second transition F_{th2} occurred characterized by the transformation of the widened quasi-percolated pattern into individual spherically shaped nanoparticles. The observed changes were induced under a single laser pulse as in the present case. The observed transitions took place upon irradiation at quite small fluences (from 25 to 35 mJ cm^{-2}); these are far below the typical ablation threshold of silver in the region below 1 J cm^{-2} [14]. In our previous work we showed that it is possible to take advantage of the laser-induced changes on individual nanoparticles to produce patterning in the nanostructured thin film by illuminating through spatially designed light fields.

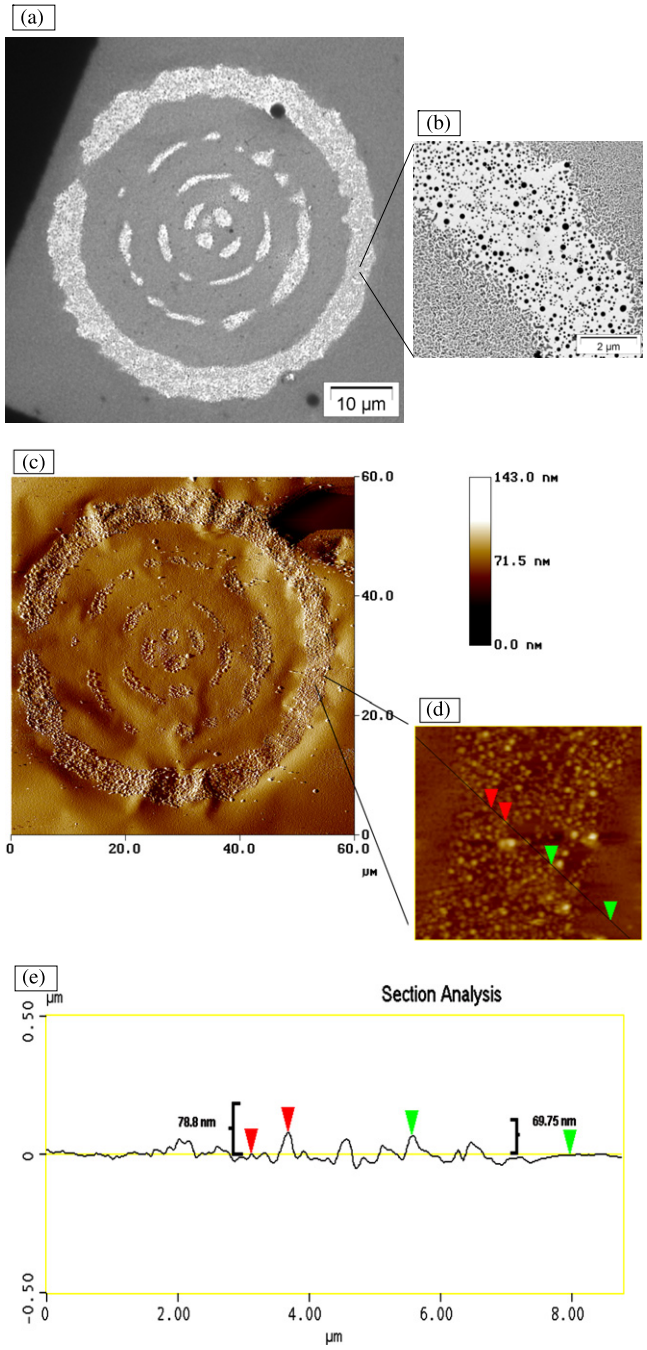

Figure 2. Circular patterns obtained upon irradiation through a pinhole with a diameter of 60 μm placed at 300 μm from the sample, visualized by TEM (a) and AFM (c), with corresponding structural details (b) and (d), respectively. The high resolution AFM image (d) shows an area of 64 μm^2, with a height scale of 0.5 μm on the cross-section profile (e).

These structured light fields can be obtained using suitable masks and gratings.

In the present investigation, we address the case of a mask with a small hole (pinhole having a diameter of 60 μm) as shown in figure 1 to generate a simple pattern resulting from its diffracted light field. In figure 2(a) the TEM image of the irradiated sample with an average fluence of $F_0 = 25$ mJ cm^{-2} is shown. The corresponding image obtained by AFM is shown in figure 2(c). The material has been modified in three concentric ring-shaped stripes of decreasing width from the exterior to the interior (labeled R_1, R_2 and R_3, respectively). The morphology between the rings corresponds to the un-irradiated region which is presented in figure 1 right-hand side (quasi-percolated state). In figure 2(b) an amplification of ring R_1 is presented. Inside the ring the material has been transformed into nanospheres having dimensions in the range between 10 and 100 nm. This transformation is associated with the second morphological transformation occurring at an irradiation threshold F_{th2} mentioned before. In both rings R_2 and R_3 the same effects are observed: however, the widths of the rings decrease. In addition, at each border of ring R_1 (see figure 2(b)), two small concentric regions can be distinguished consisting of a wider quasi-percolated pattern which is associated with an irradiation fluence just above the first threshold F_{th1} discussed above. The same changes, though less evident, can be observed in rings R_2 and R_3. The morphology at the center of the circular patterns is more complex, suggesting that the pinhole is not perfectly circular or the mask is not perfectly parallel to the sample surface. In fact, the principal problem of our experimental set-up is that the silver nanostructures are deposited on a TEM grid covered with an amorphous carbon thin film. This film is not a flat surface, therefore uniformity effects are evident in the images obtained by AFM [12]. Furthermore the rings are not complete; this is probably due again to the non-uniformity of the films. In figure 2(c) the AFM image is presented and the concentric rings R_1, R_2 and R_3 are clearly observed. The additional information in this case is the height of the transformed (and untransformed) regions as shown in figures 2(d) and (e). The AFM results are summarized in table 1. For the larger nanoparticles the diameters are in accordance with the TEM measurements. The smaller nanoparticles were more difficult to analyze by AFM, probably because of the non-uniformity of the surface underneath. However, in R_1 some measurements gave 10–30 nm in diameter and from 5–10 nm in height. It is interesting to note from table 1 that the nanoparticles have a tendency to decrease in diameter as one goes from the exterior to the interior rings. The AFM results show that the nanoparticles are not spherical but oblate (diameter > height) in the first two rings. However, in ring R_3 the opposite appears to occur (height > diameter). At this point we do not have an explanation for this effect but it indicates that the transformations are very sensitive to the changes in intensity of the diffracted light field. In the quasi-percolated region the nanoparticles have a height of the order of 25 nm on average; their morphology is more complex (finger-like). In this case one can use the Féret diameter to characterize their size which is of the order of 100 nm [13]. In our previous paper it was found that the laser energy was absorbed

Table 1. AFM measurements of the diameter and height of the nanoparticles in rings R_1, R_2 and R_3.

	R_1	R_2	R_3
Diameter (nm)	100–160	100–130	100–120
Height (nm)	75–88	80–100	143–180

mainly by the silver nanostructures rather than the carbon substrate [7]. This explanation is still valid in the present case since at this wavelength (355 nm) silver is strongly absorptive. The laser pulse induces the melting and diffusion processes reshaping the nanoparticles into truncated spheroids which are thermodynamically a more favorable morphology. It is worth mentioning that a locally laser-induced solid to liquid mechanism was invoked to explain analogous results in quasi-percolated gold thin films [10].

For some simple cases such as the patterning of silver quasi-percolated thin films through a razor edge or a single slit we have shown that the experimental results can be described using Fresnel diffraction theory [7, 11]. The case of circular apertures is mathematically more complex. To calculate the light field produced by the diffraction of a circular aperture we consider an observation point P at the plane of the sample. The sample is located at a distance Z from the source and at a distance Z_0 from the mask with a circular aperture which has a diameter a.

Starting from the Fresnel integral in polar coordinates [15, 16]:

$$U = U_0 \frac{Z+Z_0}{\mathrm{i}\lambda Z Z_0} a^2 \mathrm{e}^{\mathrm{i}\pi \frac{r^2}{\lambda Z_0}} \iint (\xi,\eta)\, \mathrm{e}^{\mathrm{i}\pi \frac{(Z+Z_0)}{Z Z_0}\rho^2} \times \mathrm{e}^{-\mathrm{i}\frac{2\pi}{\lambda Z_0} a r \rho \cos(\varphi-\theta)} \rho \,\mathrm{d}\rho \,\mathrm{d}\varphi \quad (1)$$

where $U_0 = \frac{A\mathrm{e}^{\mathrm{i}k(Z+Z_0)}}{Z+Z_0}$ is the field at the point of observation P without the mask and (ξ, η) is the complex amplitude.

This integral is solved using the Hankel transform of zero order:

$$U = U_0 \frac{Z+Z_0}{\mathrm{i}\lambda Z Z_0} a^2 \mathrm{e}^{\mathrm{i}\pi \frac{r^2}{\lambda Z_0}} \int 2\pi\rho \,\mathrm{d}\rho J_0\left[\frac{2\pi}{\lambda Z_0} a r \rho\right] \mathrm{e}^{\frac{-\mathrm{i}a^2(Z+Z_0)}{\lambda Z Z_0}\rho^2} \quad (2)$$

where the last integral that contains the Bessel function has solutions in terms of the Lomel functions.

The irradiance is given in units of U_0 and assuming in this case that the source is at $Z \gg 0$:

$$I = |U^2| = \pi^2 \frac{a^4}{\lambda^2 Z_0^2}(C^2 + S^2) \quad (3)$$

where C and S are the Lomel functions [15, 16].

The theoretical diffraction intensity profile resulting from the mask with a hole is obtained solving equation (3) and is presented in figure 3 bottom by a solid line as a function of the horizontal distance x in the plane of the sample. Using the measured experimental parameters (laser wavelength $\lambda = 355$ nm, distance from the mask to the sample $Z_0 = 300 \pm 30$ μm and diameter $a = 60$ μm of the pinhole) the oscillations of the diffracted pattern match quite well the spacing between the induced morphological rings R_1, R_2 and R_3 of the nanostructured thin film (figure 3 top). It is important to mention that in our experimental set-up Z_0 (distance from pinhole to mask) was difficult to control precisely in particular because the surface of the sample is not flat. This has consequences in the interference phenomena occurring here; one of these is that the transformed rings are not complete. We have therefore considered this distance as an adjustable parameter and we have varied it by about 10%.

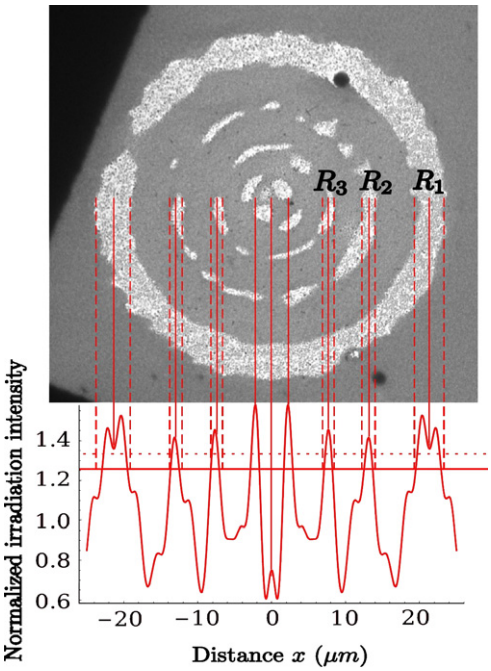

Figure 3. TEM microphotograph of the imprinted rings. The solid line is the diffracted intensity as a function of the horizontal distance x in the plane of the sample, according to Fresnel theory. The vertical dotted lines allow us to determine the minimum energy density $F_{\min}$ represented by a solid horizontal line needed to transform the quasi-percolated nanostructures into nanoparticles.

The best accordance to our experimental results (position of the diffracted intensity peaks and their corresponding width) was for $Z_0 = 306$ μm. It is thus easy to identify the diffracted intensity field associated with the observed micrograph. This is represented by the solid and dotted vertical lines. The solid vertical lines coincide with the middle of the irradiated ring, while the dotted lines with the borders of the ring. The solid horizontal line defines then the minimum energy density $F_{\min}$ necessary to transform the quasi-percolated silver into nanospheres. Using the measured experimental value for F_0 (25 mJ cm^{-2}) the threshold value can be determined. Therefore $F_{\min}/F_0 = 1.23$ and thus $F_{\min} = 30.75$ mJ cm^{-2}. This is very close to the value found in a previous work which was 28 mJ cm^{-2} irradiating with a KrF excimer laser ($\lambda = 248$ nm with a pulse duration of 25 ns) [7]. The dotted horizontal line is a guide to the eye and shows that small changes in the normalized irradiation intensity can change substantially the induced pattern in the silver thin film.

In figure 4 the theoretical diffraction intensity profile is computed for three different distances (295, 306 and 310 μm) from the pinhole to the sample. It is evident that the effect of varying this parameter is important. In the top curve of figure 4 ($Z_0 = 295$ μm) a peak is present pointing at a distance $x = 4$ μm. This peak diminishes drastically for $Z_0 = 306$ μm and completely disappears at $Z_0 = 310$ μm. This implies that a variation of 15 μm in the screen to sample distance results in drastic changes in the imprinted pattern on the quasi-percolated silver sample. In all three cases the dotted horizontal line corresponds to the threshold value

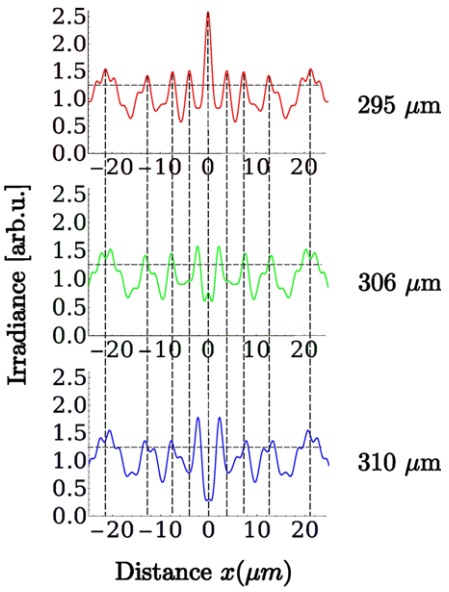

Figure 4. Diffracted intensity as a function of the horizontal distance x in the plane of the sample for three pinhole to sample distances. The dotted horizontal lines correspond to the threshold value in energy density $F_{\min}$.

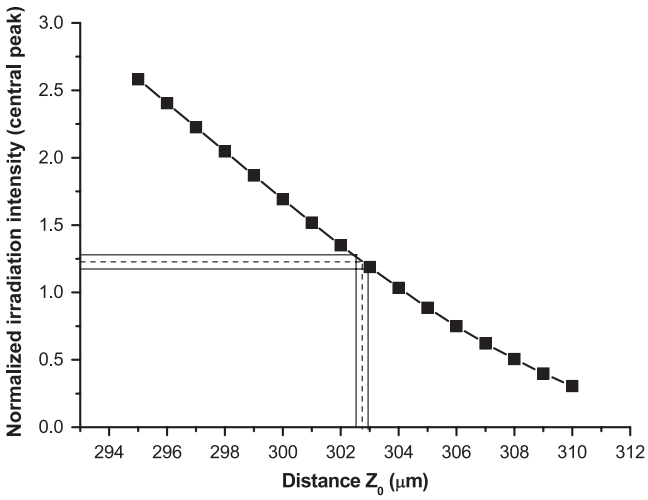

Figure 5. Diffracted intensity of the central peak as a function of the distance from the pinhole to the sample. The dotted horizontal line corresponds to the threshold value in energy density $F_{\min}$. A variation of about 500 nm in Z_0 can produce or not a mark in the center of the diffracted rings.

$F_{\min} = 30.75$ mJ cm^{-2} necessary to induce the transition from quasi-percolated nanostructures to nanoparticles. Therefore by varying the distance between the pinhole and the sample one can change the number of rings imprinted in the sample and their corresponding width.

Finally in figure 5 the variation of the normalized irradiation intensity of the central diffracted peak with the pinhole to sample distance is presented. The horizontal dotted line corresponds to $F_{\min}$ as described before. From this figure one can observe that a variation of about 500 nm around 302.7 μm in the pinhole to sample distance should result in the appearance or disappearance of a nanotransformed region in the center of the diffracted rings imprinted on the surface of the sample. This result suggests that precise patterning engineering can be achieved through the control of the spatial parameters such as the pinhole diameter and the distance from the mask to the sample.

4. Conclusions

In conclusion, we have shown that micron and submicron patterning can be achieved simultaneously by laser irradiation through a circular aperture on quasi-percolated silver thin films. Furthermore the experimental results can be explained using Fresnel diffraction theory. This suggests that nanopatterning engineering can be realized through the variation of the spatial parameters such as the diameter of the aperture and its distance to the sample. A significant improvement in the patterning quality should be achieved using very flat substrates. Further experiments are in progress.

Acknowledgments

The authors wish to acknowledge P Castillo for her technical assistance with the TEM measurements. This work was partially sponsored by the Consejo Nacional de Ciencia y Tecnología (CONACYT) of México under contract CB-2005-C01-50632-F.

References

[1] Jung Y S, Jung W and Ross C A 2008 Nanofabricated concentric ring structures by template self-assembly of a diblock copolymer *Nano Lett.* **8** 2975–81
[2] Vollmer M, Weidenauer R, Hoheisel W, Schulte U and Träger F 1989 Size manipulation of metal particles with laser light *Phys. Rev.* B **40** 12509–12
[3] Inisawa S, Sugiyama M and Koda S 2003 Size controlled formation of gold nanoparticles using photochemical growth and photothermal size reduction by 308 nm laser pulses *Japan. J. Appl. Phys.* 1 **42** 6705–12
[4] Resta V, Siegel J, Bonse J, Gonzalo J, Afonso C N, Piscopiello E and Van Tenedeloo G 2006 Sharpening the shape distribution of gold nanoparticles by laser irradiation *J. Appl. Phys.* **100** 084311
[5] Tsuji T, Iryo K, Watanabe N and Tsuji M 2002 Preparation of silver nanoparticles by laser ablation in solution: influence of laser wavelength on particle size *Appl. Surf. Sci.* **202** 80–5
[6] Qiu J, Jiang X, Zhu C, Shirai M, Si J, Jiang N and Hirao K 2004 Manipulation of gold nanoparticles inside transparent materials *Angew. Chem. Int. Edn* **43** 2230–34
[7] Haro-Poniatowski E, Lacharme J P, Fort E and Ricolleau C 2005 Patterning of nanostructured thin films by structured light illumination *Appl. Phys. Lett.* **87** 143103
[8] Van Overschelde O and Wautelet M 2006 Diffraction-aided laser-induced microstructuring of thin TiO_2 films on glass *Appl. Phys. Lett.* **89** 161114
[9] Riedel R, Hernández-Pozos J L, Palmer R E and Kolasinski K W 2004 Fabrication of ordered arrays of silicon cones by optical diffraction in ultrafast laser etching with SF_6 *Appl. Phys.* A **78** 381–5
[10] Eurenius L, Hägglund C, Olsson E, Kasemo B and Chakarov D 2008 Grating formation by metal–nanoparticle-mediated coupling of light into waveguide modes *Nat. Photon.* **2** 360–4

[11] Alonso-Huitrón J C, Acosta-Zepeda C, Batina N, Acosta-García M C, Castillo-Ocampo P and Haro-Poniatowski E 2009 UV-laser induced modifications through a single slit on quasi-percolated silver nanostructured films *Radiat. Eff. Defects Solids* **164** 438–42

[12] Haro-Poniatowski E, Batina N, Acosta-García M C, Pohl-Alfaro M A, Castillo-Ocampo P, Ricolleau C and Fort E 2007 UV laser radiation effects on silver nanostructures *Radiat. Eff. Defects Solids* **162** 491–9

[13] Alonso J C, Diamant R, Castillo P, Acosta-García M C, Batina N and Haro-Poniatowski E 2009 Thin film silver nanoparticles deposited in vacuum by pulsed laser ablation using a YAG:Nd laser *Appl. Surf. Sci.* **255** 4933–7

[14] Svendsen W, Schou J, Thestrup B and Ellegaard O 1996 Ablation from metals induced by visible and UV laser irradiation *Appl. Surf. Sci.* **96–8** 518–21

[15] Born M and Wolf E 1999 *Principles of Optics* 7th edn (expanded) (Cambridge: Cambridge University Press) chapter VIII pp 484–92

[16] Mielenz K 1998 Algorithms for Fresnel diffraction at rectangular and circular apertures *J. Res. Natl. Inst. Stand. Technol.* **103** 497–509